SEAWEED AND SEAGRASS MAPPING IN THAILAND MEASURED USING LANDSAT 8 OPTICAL AND TEXTURAL IMAGE PROPERTIES

Satomi Kakuta
Research and Development Institute, Asia Air Survey Co., Ltd., stm.kakuta@ajiko.co.jp

Wataru Takeuchi
Institute of Industrial Science, University of Tokyo, Japan.

Anchana Prathep
Department of Biology, Faculty of Science Prince of Songkla University, Thailand

SEAWEED AND SEAGRASS MAPPING IN THAILAND MEASURED USING LANDSAT 8 OPTICAL AND TEXTURAL IMAGE PROPERTIES

Satomi Kakuta[1], Wataru Takeuchi[2], and Anchana Prathep[3]

ABSTRACT

Seaweed and seagrass beds are an important ecosystem in coastal zones. However, they are degrading because of various causes, such as the anthropogenic impacts of coastal development, aquaculture, overharvesting, and climate change. To contribute to the research related to coastal blue carbon and marine biodiversity as well as conservation and sustainable management of natural resources in coastal regions, the spatial distribution of benthic cover derived from satellite images can be the most practical tool for monitoring seaweed and seagrass beds. This study aimed at mapping the latest distribution of seaweed and seagrass in Thailand using Landsat 8 images. Thus, we developed a classification method that includes regional segmentation by ISODATA clustering, analysis of optical and textural properties, and classification using a decision tree. First, a subset of images, including those of the Sirinat National Park in Phuket, Southern Thailand, was extracted from the Landsat 8 full-scene images as a training site for the development of a classification method. Then, the developed method was evaluated by comparing the classification result to a visual interpretation result. The classification and visual interpretation results were found to be consistent to each other with a 98% total accuracy. Next, the method was applied to the Landsat 8 full-scene image, and quality assessment was conducted at two different water-type areas: Patong Beach and Tang Ken Bay. At Patong Beach, which has clear seawater, the classification result was consistent with the result of the training site. However, in the Tang Ken Bay, where the seawater is turbid, misclassification of the result evidently occurred. It is believed that the segmentation sizes were not appropriate for benthic cover distributed over small areas,

and that the thresholds utilized in the decision tree were not suitable for turbid water.

I. INTRODUCTION

Seaweed and seagrass beds are well known as an important ecosystem in coastal zones through variety of functions, such as nurseries, shelters, and foods (Prathep, 2005; Adulyanukosol and Poovachiranon, 2006; Prathep et al., 2010; Petsut et al., 2012). However, they are degrading because of various causes, such as the anthropogenic impacts of coastal development, aquaculture, overharvesting, and climate change (Prathep et al., 2010; Petsut et al., 2012). The spatial distribution of benthic cover derived from satellite images can contribute to the research related to coastal blue carbon (Prathep, 2012) and marine biodiversity as well as conservation and sustainable management of natural resources in coastal regions. Therefore, this study aims to map the latest distributions of seaweed and seagrass in Thailand using Landsat 8 images.

In recent similar studies, Tamondong et al. (2013) showed that benthic cover can be accurately classified into dense and less dense seagrass, sand/rubbles, and corals/seaweed using high-resolution multispectral data. Water column correction using bathymetric data was necessary for accurate classification. Yahya et al. (2010), Komatsu et al. (2012), and Noiraksar et al. (2014) introduced the depth invariant index (DII) proposed by Lyzenga (1981) to benthic cover classification, such as for the identification of seaweed and seagrass. DII suitably corrects water column effects without requiring bathymetric data. However, there is a limitation to the accurate classification of benthic cover because the data used for classification (DII) is only one dimensional. Roelfsema et al. (2013) showed that benthic cover can be classified into seven categories, including seagrass species and density, by object-based classification using high-resolution multispectral data without water column correction. Although Lyons et al. (2010) also applied object-based classification to middle resolution multispectral data, benthic cover was classified into only three categories of seagrass density. It has not been proven that object-based classification is appropriate to middle resolution data for benthic cover classification. In addition, object-based techniques are not generalized for wide use because

they rely somewhat on the functions of the specific application software.

The mapping method being developed in this study can be applied to middle resolution data, accurately classifying benthic types such as seagrass, seaweed, and coral reefs. By applying water column correction without utilizing bathymetric data for considering limited information, the method can map sustainably using common rules based on an understanding of the optical and textural properties of seagrass and seaweed.

We propose a classification method that includes ISODATA clustering, analysis of optical and textural properties, and classification using a decision tree. In this paper, we show investigative results by applying the method to study sites in Phuket, Southern Thailand.

II. METHODOLOGY

1. Study Site and Data

The study site was selected in the coastal region, including Sirinat National Park in Phuket, Southern Thailand. The seawater is clear because sediment does not run off, and seagrass habitats are widely distributed. The satellite data utilized for this study were Landsat 8 OLI, Level 1T products (geometrically corrected using DEM and GCPs), which were acquired on December 23, 2013 and downloaded from the U.S. Geological Survey. The data were selected under the conditions of least cloud cover and lowest effect of sun glare among all scenes in the past year.

2. Pan-Sharpening and Masking

Fig. 1 shows a flowchart of the data analysis. Before starting this analysis, the geometric accuracy of the Landsat data was examined by comparing them with SWBD (SRTM Water Body Data). Then, pan-sharpening was performed in order to extract the benthic texture properties. For this process, band 2 (450-515 nm), band 3 (525-600 nm), and band 4 (630-680 nm) were utilized along with band 8 (500-680 nm). These bands were selected for conditions in which both the multispectral and panchromatic bands could detect reflectance from seafloors, and the spectral wavelength range of the panchromatic band fully covered the total range of multispectral bands because consistency in the ranges of these bands is necessary for avoiding spectral distortion. Likewise, band 1 (433-453 nm) was excluded because its spectral wavelength range was beyond of the range of band 8. Principal Component Analysis was adopted as a pan-sharpening technique that retains the original spectral characteristics (Kakuta et al., 2014). Meanwhile, mask data for land and deeper water were created from the multispectral data in order to extract shallow water. At first, a gray-level image was created by computing an equation (band 5-band 3) / (band 5 + band 3) that enhances the contrast between water and other features. Then, image-thresholding was applied to the gray-level image to create a binary image (land mask). A deeper water mask was created using a 3-km buffer toward the ocean from the coastlines of the land mask.
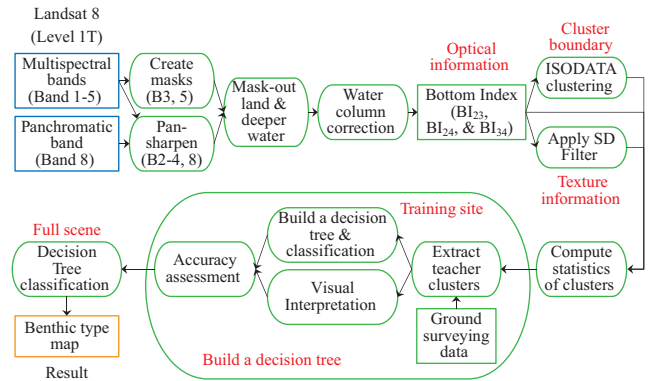

Fig. 1. Flowchart of the data analysis.

3. Water Column Correction

After extracting the shallow water, water column correction was performed on pan-sharpened data by computing the Bottom Index (BI) (Matsunaga et al., 2000), which is an algorithm developed based on the Lyzenga equation (1978) to minimize the water depth effect on the satellite data. BI is given by the following equation:

$$BI_{ij} = \ln(L_i - L_{\infty i}) - k_{ij} * \ln(L_j - L_{\infty j}) \qquad (1)$$

where i and j are band numbers. BI_{ij} is BI computed from a combination of bands i and j. L_i and L_j are pixel values of bands i and j. $L_{\infty i}$ and $L_{\infty j}$ are constant values of bands i and j to remove both the path radiance and electronic offsets. k_{ij} is an extinction coefficient ratio of bands i to j. k_{ij} is determined as a gradient given by a regression analysis between two bands. L_i and L_j, the pixel values used for the regression analysis, were sampled at the sand bottom at various depths, and natural logarithms were applied after removing any offsets. The sand bottom was sampled by transecting the coasts in the study area through visual interpretation. $L_{\infty i}$ and $L_{\infty j}$, the constant values used to remove both the path radiance and electronic offsets, were determined as values of the left ends of the histograms of bands i and j for the whole masked-out land image. In this study, all combinations of bands 2, 3, and 4, to which pan-sharpening was already applied, were utilized (bands i and j as are indicated as BI_{ij}).

4. Regional Segmentation by ISODATA Clustering

Regional segmentation in shallow water was performed by the ISODATA clustering technique using BI_{23}, BI_{24}, and BI_{34}. The ISODATA clustering technique was adopted because it is one of classic and practical methods for regional segmentation that groups similar colored pixels into a cluster. Before processing the clusters, BI_{23}, BI_{24}, and BI_{34} were treated with a smoothing filter in order to remove noise and reduce small clusters. The smoothing filter was implemented by computing the median values of local moving windows (7×7) in a full image. The window size was the largest size for the condition in which segments, including seagrass areas, could be separated from sand or rocks

by ISODATA clustering. Seagrass and seaweed were sometimes classified into the same category by applying ISODATA clustering because they indicate similar optical properties. However, there was a possibility that seagrass and seaweed could be distinguished from each other based on the different conditions of those habitats. Therefore, non-neighboring clusters classified into a same category were separated from each other and classified based on textural properties.

In the next step, BI_{23}, BI_{24}, and BI_{34} not treated with a smoothing filter were treated with a standard deviation (SD) filter in order to extract the benthic textural properties. The SD filter was implemented by computing the SD values of local moving windows (3×3) in a full image. The SD value in each local window represented the non-uniformity of brightness, which equally indicated a spatial heterogeneous distribution of benthic types. The window size was the smallest size to minimize image blurring. After that, statistics for all clusters were computed using BI_{23}, BI_{24}, and BI_{34} not treated with the smoothing filter and those BIs treated with the SD filter.

5. Decision Tree Classification

A training site that included Sirinat National Park in Phuket was separated from the full scene in order to build a decision tree. Clusters of seagrass, coral reefs, sand, and ocean (water surface without reflection from sea floors) were identified and extracted from the subset image by referencing ground survey data in 2014 (called "teacher clusters"). A decision tree for benthic type classifications was built from teacher cluster statistics by understanding the optical and textural properties.

By using the decision tree and cluster statistics, benthic types at the training site were classified into the four categories of seagrass, coral reefs, sand, and ocean. Thresholds in the decision tree were derived objectively in order to be generally applied to other areas. The benthic type classification result was qualitatively compared with a visual interpretation result of ISODATA clusters. A quantitative comparison was also performed using a confusion matrix with a pixel base.

After examining the validity of the decision tree by accuracy assessment, a benthic type map was obtained by applying the decision tree to the full scene.

III. RESULTS AND DISCUSSION

1. Optical and Textural Properties of Benthic Types

Fig. 2 shows (a) a pan-sharpened false color composite image, (b) BI color composite image and approximate locations of benthic types, and (c) BI color composite image treated with an SD filter. Differences between the benthic types can be easily recognized by the different color tones in (b), whereas the differences can hardly be recognized in (a). Differences between the seagrass and coral ridge can be recognized in (c). These features were examined using the teacher cluster statistics.

Fig. 3 shows normalized mean value of teacher clusters in (a) BI and (b) BI treated with an SD filter. The mean values of BI and BI treated with an SD filter were normalized for (a) and
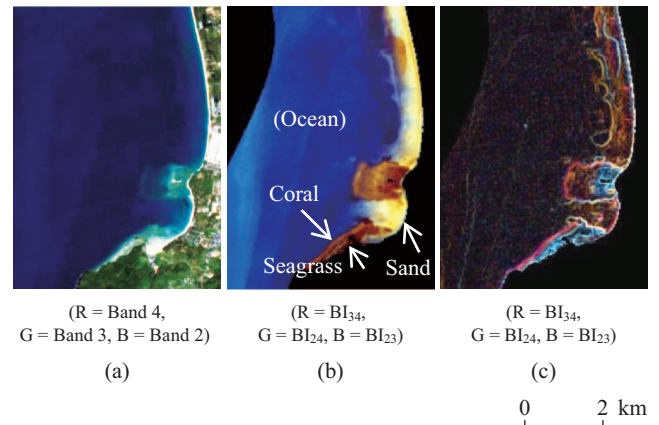

(a) (R = Band 4, G = Band 3, B = Band 2) (b) (R = BI_{34}, G = BI_{24}, B = BI_{23}) (c) (R = BI_{34}, G = BI_{24}, B = BI_{23})

0   2 km

Fig. 2. Training site: (a) pan-sharpened false color composite image, (b) BI color composite image, (c) BI color composite image treated with SD filter.
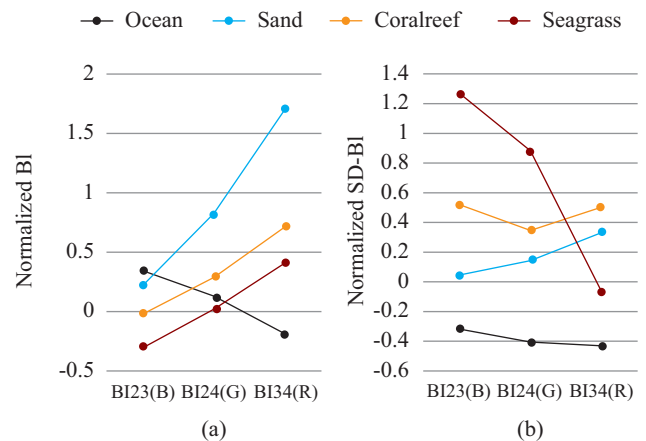

Fig. 3. Normalized mean values of teacher clusters in (a) BIs and (b) BIs treated with SD filter.

(b) in order to standardize the dynamic range in each BI by computing $(\mu - \mu_0) / \sigma_0$, where μ is the mean value of a cluster, μ_0 is the mean value of all clusters, and σ_0 is the standard deviation of all clusters.

In Fig. 3(a), there is a tendency for the mean values of ocean to be the highest in BI_{23} (B) and the lowest in BI_{34} (R) among all benthic types. By contrast, there is a tendency for the mean values of sand, coral reef, and seagrass to show opposite patterns to those of ocean in BI_{23} (B) and BI_{34} (R). These tendencies are consistent with Fig. 2(b).

In Fig. 3(b), there is a tendency for the mean values of seagrass to be the highest in BI_{23} (B) and BI_{24} (G) and lower in BI_{34} (R) among all benthic types. By contrast, there is a tendency for the mean values of coral reef to show opposite patterns to those of seagrass in BI_{23} (B), BI_{24} (G), and BI_{34} (R). These tendencies are consistent with Fig. 2(c).

2. Classification Results Using Decision Tree

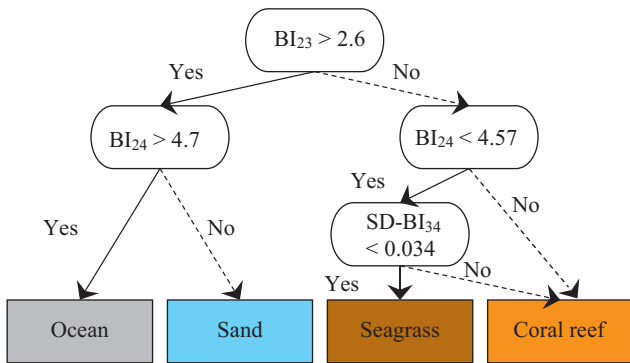The decision tree shown in Fig. 4 was built based on the

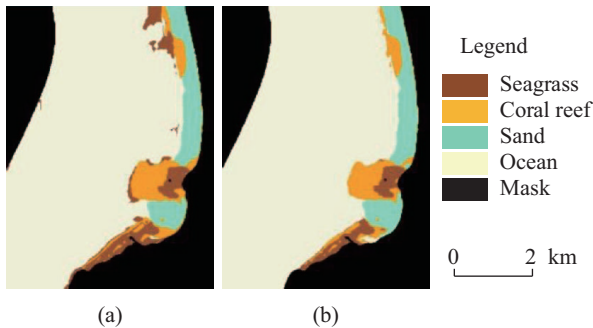**Fig. 4. Decision tree for benthic type classification.**

Fig. 5. (a) A benthic type classification result using decision tree and (b) a visual interpretation result of ISODATA clusters.

Table 1. A comparison of the benthic type classification result with the visual interpretation result.

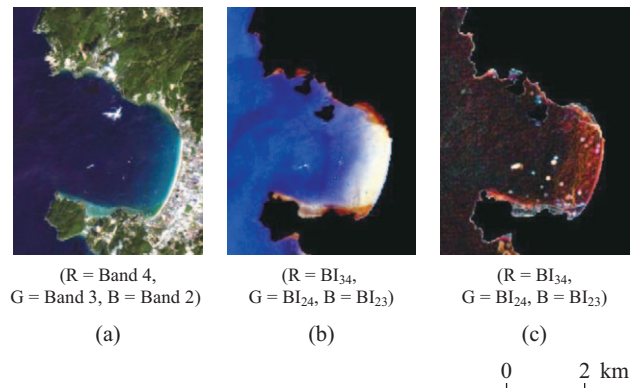| Accuracy		DT-Classification				Total (pix)	PA
		Seagrass	Coral reef	Sand	Ocean		
Interpre- tation	Seagrass	3,582	235	9	0	3,826	**94%**
	Coral reef	802	6,082	53	3	6,940	**88%**
	Sand	2	388	9,815	0	10,205	**96%**
	Ocean	292	231	36	92,251	92,810	**99%**
Total (pix)		4,678	6,936	9,913	92,254	113,781	
UA		**77%**	**88%**	**99%**	**100%**		**98%**

Fig. 6. Patong Beach: (a) pan-sharpened false color composite image, (b) BI color composite image, (c) BI color composite image treated with SD filter.
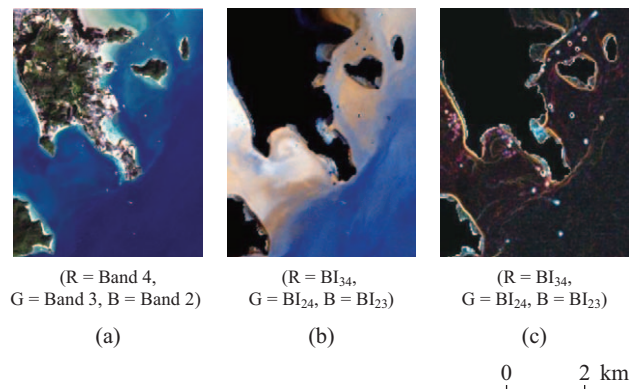

Fig. 7. Tang Ken Bay: (a) pan-sharpened false color composite image, (b) BI color composite image, (c) BI color composite image treated with SD filter.

properties of the teacher clusters. BI_{23} and BI_{24} indicated in the decision tree are the mean values of each cluster in BI_{23} and BI_{34}, respectively. SD-BI34 is the mean value of each cluster in BI_{34} treated with an SD filter. All thresholds were computed using the Otsu method (Otsu, 1979). Fig. 5 shows (a) a benthic type classification result using the decision tree and (b) a visual interpretation result of ISODATA clusters based on the properties of teacher clusters. The interpretation result was used for accuracy assessment.

3. Accuracy Assessment of Training Site

According to Fig. 5, seagrass in deeper water is classified in the classification result. However, it is not classified in the interpretation result. Except for the partial differences, the distributions of all benthic types are nearly identical.

Table 1 shows a confusion matrix for quantitative comparison of the benthic type classification result with the visual interpretation result. Producer's accuracy (PA) is a percentage of the number of correctly classified pixels to the number of all interpreted pixels in a benthic type. User's accuracy (UA) is a percentage of the number of interpreted pixels to the number of all classified pixels in a benthic type. The value in the bottom right cell of the table is the total accuracy, which is a percentage of the total number of correctly classified pixels to the total number of pixels. As a result, the UA of seagrass has a lower accuracy (77%) than the others because the classified seagrass

included interpreted coral reef. However, the total accuracy (98%), PA of all benthic types (more than 88%), and UA except seagrass (more than 88%) have very high accuracy; therefore, it was confirmed that the classification result is valid.

4. Benthic Type Map for Other Areas: Patong Beach and Tang Ken Bay

After examining the validity of the decision tree, a benthic type map was obtained by applying the decision tree to the full scene. The thresholds were not recomputed for the full scene.

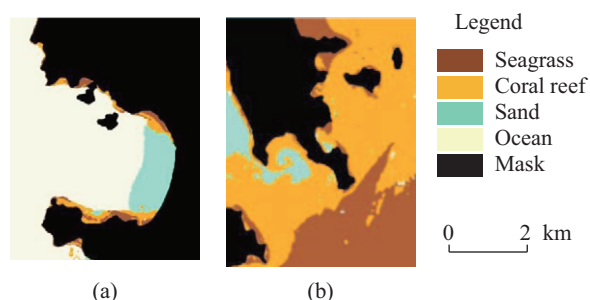Figs. 6 and 7 show (a) a pan-sharpened false color composite

Legend
- Seagrass
- Coral reef
- Sand
- Ocean
- Mask

0   2 km

(a)   (b)

Fig. 8. Benthic type classification result from (a) Patong Beach and (b) Tang Ken Bay.

image, (b) BI color composite image, and (c) BI color composite image treated with an SD filter at Patong Beach and Tang Ken Bay, respectively. There are significant differences in color tones between Figs. 6(b) and 7(b), whereas no great differences in the tendencies of color tone or texture are found in pairs 6(a), 7(a) and 6(c), 7(c), except that the color tone in 7(a) is brighter than in 6(a).

Fig. 8 shows the benthic type classification results for (a) Patong Beach and (b) Tang Ken Bay. The benthic type distribution in Fig. 8(a) is consistent with the classification result for the training site, whereas 8(b) is evidently misclassified. It is believed that there are two reasons why seagrass and coral reef were misclassified despite the fact that those distributions could be visually recognized in Figs. 7(b) and 7(c). The first reason is that the seagrass distribution areas were very small. Seagrass areas were merged with other neighboring benthic cover clusters, such as sand, after smoothing filtering and ISODATA clustering. The statistics for clusters including seagrass indicated different values from those of the seagrass teacher clusters. Consequently, those clusters were misclassified. The second reason why coral reef caused misclassification is that the statistics for those clusters indicated different values from those of the teacher clusters after being affected by turbid water, even though coral reef areas were successfully clustered. Accordingly, improvement in the developed method is needed so that it can apply not only to clear water but also to turbid water. For improvement of the misclassified area, a different set of extinction coefficient ratio k_{ij} and thresholds is needed in the decision tree for turbid water (Fig. 4). Moreover, prior to classification, the entire image needs to be separated into two or more parts, where the value of k_{ij} is assumed homogeneous. For future work, a pre-computed database for the determination of k_{ij} and decision tree thresholds needs to be developed for several types of water in Thailand.

IV. CONCLUSIONS

A method for benthic type classification was developed for seaweed and seagrass mapping at the study site under suitable conditions in Phuket, Southern Thailand. The validity of the method was confirmed by comparing the classification result with a visual interpretation result from ISODATA clusters. The ac-

curacy assessment indicates that the classification result is valid with a total accuracy of 98%. After examining the validity of the decision tree, a benthic type map was obtained by applying the decision tree to the full scene. The classification results were examined in other areas: Patong Beach and Tang Ken Bay. At Patong Beach, where the seawater is clear, the site was classified as it was for the training site. However, the other site was evidently misclassified. It is believed that regional segmentation by ISODATA clustering after treatment with a smoothing filter was not appropriate for benthic cover distributed over small areas. In addition, the thresholds utilized in the decision tree were not appropriate for turbid water. For future work, there is a possibility that benthic cover such as seagrass distributed with small areas can be correctly classified when those areas are classified using optical information after extraction using textural information. Moreover, a pre-computed database for the determination of k_{ij} and the decision tree thresholds needs to be developed for several types of water in Thailand.

REFERENCES

Adulyanukosol, K. and S. Poovachiranon (2006). Dugong (Dugong dugon) and seagrass in Thailand: present status and future challenges. Proc. 3rd Int. Symp. SEASTAR and Asian Bio-logging Science, 41-50.

Kakuta, S., W. Takeuchi and A. Prathep (2014). Seaweed and seagrass mapping in Thailand measured by using Landsat 8 optical properties. Proc. The International Bioscience Conference and the 5th Joint International PSU-UNS Bioscience Conference 2014, T1-O14.

Komatsu, T., T. Noiraksar, S. Sakamoto, S. Sawayama, H. Miyamoto, S. Phauk, P. Thongdee, S. Jualaong and S. Nishida (2012). Detection of seagrass beds in Khung Kraben Bay, Thailand, using ALOS AVNIR2 image. Proc. of SPIE Vol. 8527 85270I-1.

Lyzenga, D. R. (1978). Passive remote sensing techniques for mapping water depth and bottom features. Applied Optics 17, 379-383.

Lyzenga, D. R. (1981). Remote Sensing of Bottom Reflectance and Water Attenuation Parameters in Shallow Water Using Aircraft and Landsat Data. Int. J. Remote Sensing 2, 71-82.

Lyons, M. B., S. R. Phinn and C. M. Roelfsema (2010). Long term monitoring of seagrass distribution in Moreton Bay, Australia, from 1972-2010 using Landsat MSS, TM, ETM+. Proc. Geoscience and Remote Sensing Symposium (IGARSS), 2010 IEEE International, 5-8.

Matsunaga, T., A. Hoyano and Y. Mizukami (2000). Monitoring of coral reefs on Ishigaki Island in Japan using multitemporal remote sensing data. Proc. SPIE 4154, 212-222.

Noiraksar, T., S. Sawayama, S. Phauk and T. Komatsu (2014). Mapping Sargassum beds off the coast of Chon Buri Province, Thailand, using ALOS AVNIR-2 satellite imagery. Botanica Marina 57(5), 367-377.

Otsu, N. (1979). A threshold selection method from gray-level histograms. IEEE Trans. Syst., Man, Cybern., SMC-9, 62-66.

Petsut, N., A. Chirapart and M. Keawnern (2012). A stability assessment on seasonal variation of seaweed beds in the Trat peninsula of Thailand. Biodiversity Journal 3(3), 229-236.

Prathep, A. (2005). Spatial and temporal variations in diversity and percentage cover of macroalgae at Sirinat Marine National Park, Phuket province, Thailand. Science Asia 31, 225-233.

Prathep, A., E. Rattanachot and P. Tuntiprapas (2010). Seasonal variations in seagrass percentage cover and biomass at Koh Tha Rai, Nakhon Si Thammarat Province, Gulf of Thailand. Songklanakarin J. Sci. Technol. 498 32(5), 497-504.

Prathep, A. (2012). Seagrass bed as a Carbon Sink in Ranong Biosphere Reserve and Trang-Haad Chao Mai Marine National Park; an important role of seagrass. Man Bioshere (MAB) Program, UNESCO, available at: http://

www.unesco.org/new/fileadmin/MULTIMEDIA/HQ/SC/pdf/Final_report_
Anchana_Prathep.pdf (last access: 17 May 2015).

Roelfsema, C., M. Lyons, E. Kovacs, S. Phinn and M. Dunbabin (2013). Mapping changes in seagrass properties from high spatial resolution satellite image data: 2004-2013. Abst. Geoscience and Remote Sensing Symposium (IGARSS), 2013 IEEE International.

Tamondong, A. M., A. C. Blanco, M. D. Fortes and K. Nadaoka (2013). Mapping of seagrass and other benthic habitats in Bolinao, Pangasinan using Worldview-2 satellite image. Proc. Geoscience and Remote Sensing Symposium (IGARSS), 2013 IEEE International, 1579-1582.

Yahya, N. N., M. I. S. Mohd, S. Ahmad and T. Komatsu (2010). Seagrass and seaweed mapping using ALOS AVNIR-2 and Landsat-5 TM satellite data. Proc. MRSS 2010, PWTC, Malaysia. April 28-29, 2010.